Fine-structure energies for the $1s2s\ ^3S-1s2p\ ^3P$ transition in heliumlike Ar^{16+}

K. W. Kukla and A. E. Livingston
Department of Physics, University of Notre Dame, Notre Dame, Indiana 46556

J. Suleiman, H. G. Berry,* R. W. Dunford, D. S. Gemmell, and E. P. Kanter
Physics Division, Argonne National Laboratory, Argonne, Illinois 60439

S. Cheng and L. J. Curtis
Department of Physics, University of Toledo, Toledo, Ohio 43606
(Received 2 September 1994)

We have measured the $1s2s\ ^3S_1-1s2p\ ^3P_0$ and $1s2s\ ^3S_1-1s2p\ ^3P_2$ fine-structure transition wavelengths in the heliumlike Ar^{16+} ion using the beam-foil spectroscopy technique with position-sensitive photon detection. The wavelength results are 559.944(16) Å for the $J=1$–2 transition and 661.533(18) Å for the $J=1$–0 transition, which correspond to measurement precisions of about 2×10^{-5} a.u. in the transition energies. These values are sensitive to the relativistic contributions in the transition energies to <500 ppm and to the total QED corrections to $<0.5\%$. The measurements confirm the significance of $(Z\alpha)^4$-dependent relativistic corrections to the $n=2$ state fine structures suggested by recent calculations. The small remaining discrepancies between these measurements and the accurate theoretical values suggest that the magnitude of uncalculated higher-order QED terms is about $0.15(Z\alpha)^4$ a.u. Our experimental results disagree with an earlier recoil-ion measurement for the $^3S_1-{}^3P_0$ transition wavelength.

PACS number(s): 31.30.Jv, 32.30.Jc, 34.50.Fa, 29.40.Gx

I. INTRODUCTION

Heliumlike atomic systems represent a fundamental testing ground for *ab initio* calculations of the fully relativistic electromagnetic interaction between charged particles in a many-body system. Two-electron ions are among the simplest systems in which the understanding of the quantum field theoretical treatment of a bound system of many particles still poses interesting unsolved problems. The energies of the low-lying states of heliumlike ions have been the focus of extensive calculations and measurements over the past two decades. In particular, the $1s2p\ ^3P_2$ and $^3P_0$ states and the $1s2s\ ^3S_1$ state possess relatively long lifetimes even in the highly charged ions (see Fig. 1). The resulting narrow linewidths allow accurate spectroscopic wavelength measurements to be performed for the $1s2s\ ^3S_1-1s2p\ ^3P_{0,2}$ fine-structure transitions, which provide strong tests of the heliumlike atomic structure calculations.

Precise variational calculations of the energies of low-lying S and P states in heliumlike ions with $Z\le10$, including the dominant relativistic corrections, were carried out by Accad, Pekeris, and Schiff in 1971 [1]. An extension of these calculations for the $n=1$ and 2 states for $Z=2-100$ was formulated by Drake [2], whose benchmark unified method combines variational techniques and the relativistic $1/Z$ expansion. A similar perturbation-expansion technique was applied by DeSerio *et al.* [3] for the $2\ ^3S-2\ ^3P$ transitions for $Z\le26$. Multiconfiguration Dirac-Fock (MCDF) calculations have been reported by Hata and Grant [4] and by Indelicato *et al.* [5] for selected ions up to $Z=54$. The unified method of Drake omitted some terms of order $(Z\alpha)^4$ a.u. and higher in both the relativistic and the QED corrections to the energies. The estimated uncertainty due to these uncalculated terms was $\pm0.2(Z\alpha)^4$ a.u. or $\pm1.2(Z/10)^4\ \mathrm{cm}^{-1}$ [2].

We have recently presented [6] a comparison of experiment with theory for the $1s2s\ ^3S_1-1s2p\ ^3P_{0,2}$ transition energies in all heliumlike ions for which accurate experiments exist from $Z=2-92$. We concluded that although no significant discrepancy appears between experiment and the unified calculations for the $^3S_1-{}^3P_2$ transition, a systematic deviation from the calculations of approximately $\sim2.3(Z/10)^4\ \mathrm{cm}^{-1}$ exists for the $^3S_1-{}^3P_0$ transition. This conclusion is consistent with the results of a new generation of accurate relativistic calculations of the heliumlike $n=2$ state structure. These theoretical approaches include the many-body perturbation theory (MBPT) technique of Johnson and Sapirstein [7] for $Z=10-36$, the configuration interaction (CI) method of Chen, Cheng, and Johnson [8] for $Z=5-100$, and the many-body all order (MBAO) procedure of Plante, Johnson, and Sapirstein [9] for $Z=3-100$. An indication of this stronger sensitivity of the $1s2p\ ^3P_0$ state energy to higher-order relativistic contributions was suggested by the relative magnitudes of terms in the perturbation-expansion calculations of DeSerio *et al.* [3].

In the present work, we have chosen to measure the $1s2s\ ^3S_1-1s2p\ ^3P_{0,2}$ transition energies in the heliumlike ion Ar^{16+} in order to provide a test of the new calculations at the level of $<0.5(Z/10)^4\ \mathrm{cm}^{-1}$, or $<0.1(Z\alpha)^4$

*Present address: Department of Physics, University of Notre Dame, Notre Dame, IN 46556.

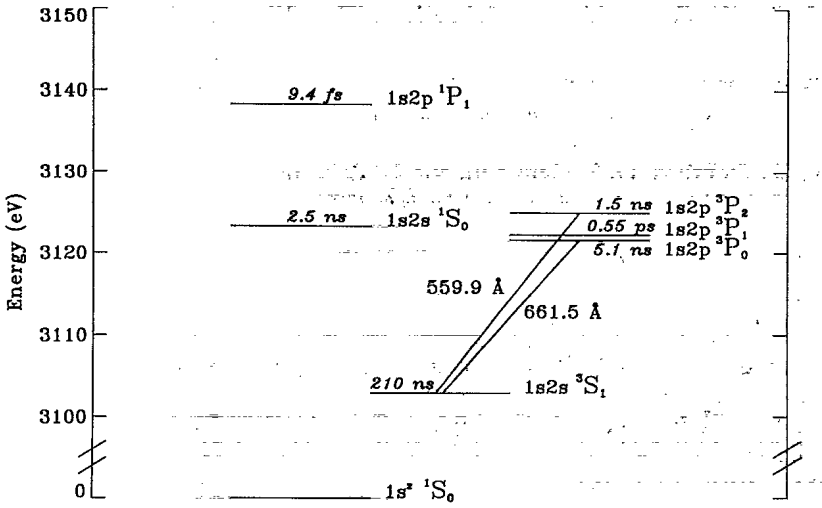

FIG. 1. Energy levels for the $n=1$ and $n=2$ states of heliumlike argon. The lifetimes of excited states are indicated, as are the $1s2s\ ^3S_1-1s2p\ ^3P_{0,2}$ transitions studied in this experiment.

a.u., as well as to resolve a discrepancy between the calculations and a previous measurement. The two previous measurements of the $^3S-^3P$ transition wavelengths in heliumlike argon are an early beam-foil spectroscopy study by Davis and Marrus [10] and a recoil-ion spectroscopy study by Beyer, Folkmann, and Schartner [11]. The beam-foil measurement was a pioneering investigation of the $2s-2p$ transitions at high Z, but with modest instrumentation and low precision. The recoil-ion study was based upon identification of weak features in a complex spectrum produced using collisional excitation of argon gas by energetic heavy ions. The recoil-ion result for the $^3S_1-^3P_0$ transition wavelength disagrees by several standard deviations with the value expected from the recent calculations and from our isoelectronic predictions [6].

The present study utilized the beam-foil fluorescence technique with position-sensitive photoelectric detection to provide the first unambiguous high resolution spectroscopic observation of the $1s2s\ ^3S_1-1s2p\ ^3P_{0,2}$ fine-structure transition wavelengths in the heliumlike Ar^{16+} ion. Our experimental results determine the $^3S_1-^3P_{0,2}$ fine-structure transition energies to <30 ppm, and they are sensitive to the total QED contributions to $<0.5\%$. We confirm the importance of new $(Z\alpha)^4$-dependent relativistic corrections to the $n=2$ state fine structure provided by recent calculations, and our results establish a limit to the size of uncalculated higher-order QED corrections for $Z=18$.

II. EXPERIMENT

The emission spectrum of highly ionized argon was produced using excitation of a fast beam of argon ions by passage through a thin solid target. The electron-cyclotron-resonance ion-source injector at Argonne National Laboratory provided a beam of Ar^{9+} ions, which were accelerated to 160-MeV energy in the ATLAS linear accelerator system. The collimated beam was directed

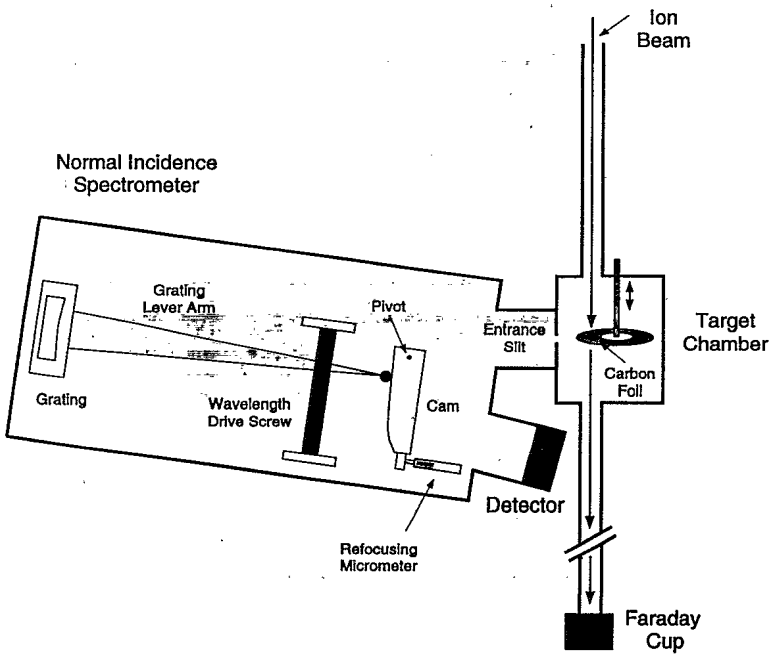

FIG. 2. Schematic diagram of the experimental setup.

through a 100-$\mu g/cm^2$ carbon foil target and was stopped in a remote shielded Faraday cup (see Fig. 2). Typical beam currents on target were 50 particle nA.

The foil-excited fluorescence spectrum of highly ionized argon was observed perpendicular to the beam direction using a 1-m, normal incidence, vacuum ultraviolet (vuv) grating spectrometer located immediately downbeam of the target. The spectrometer was refocused [12] to compensate for the ~5-Å spread of Doppler-shifted wavelengths accepted from the fast beam ($\beta=0.093$) source by the $f/10$ spectrometer. This required an increase in the optical path length within the spectrometer, which was accomplished by repositioning the grating a (wavelength-dependent) distance of about 2 cm behind its standard location. The achievable linewidth was reduced in this way to <1 Å in first order. The 1200-lines/mm grating provided a wavelength dispersion of 8.3 Å/mm in the first order of diffraction. The grating was blazed for maximum efficiency near 2500 Å, and was overcoated with osmium to enhance the reflectivity for wavelengths below 1000 Å appearing in multiple orders of diffraction. This enabled us to observe transitions in Ar^{14+} to Ar^{17+} ions possessing first-order wavelengths between 350 and 1100 Å that appeared in the second through eighth orders of diffraction at wavelengths between 1900 and 2900 Å. The corresponding higher-order linewidths ranged from about 0.5 to <0.2 Å.

The vuv spectrum was collected on a microchannel-plate (MCP) position-sensitive photoelectric detector (PSD) located in the exit plane of the spectrometer. The PSD enabled us to collect spectroscopic data simultaneously over a range of about 300 Å in first order. This not only enhanced the data collection efficiency, but also provided uniform sensitivity to time-dependent variations in the source or detector systems. The PSD assembly consisted of a pair of 40-mm-diameter MCP's with a resistive anode position encoder, operated as a one-dimensional device. The two position-sensing output voltage pulses from the anode were accumulated by computer in event mode to allow subsequent replay of the data. A timing pulse was taken from the output of the second MCP to enable signal gating. The 12.5-MHz time structure of the ATLAS beam provides the capability for eliminating a large fraction of the background signals with appropriate timing electronics and sufficient timing resolution in the detector. Our timing resolution of about 2 ns in the PSD signals coupled with the 500-ps width of the beam pulse allowed us to gate out more than 90% of the random background signals, such as detector dark counts. A more significant background effect arose from beam-induced energetic gamma rays that penetrated the chamber walls and shielding to trigger the detector with a well-defined time structure. In Fig. 3 the time spectrum of detected signals is displayed over the 80-ns time interval between beam pulses. The earlier of the two main peaks represents "prompt" gamma rays produced by the beam pulse at the target foil, which reach the detector located 30-cm away in about 1 ns. The later peak contains predominantly the vuv photon signals, delayed by nearly 6 ns with respect to the prompt gammas due to the 2-m distance the vuv photons travel through the spectrometer. The timing resolution was sufficient to eliminate the prompt gammas from our data by setting a timing acceptance window that excluded the prompt peak. However, nearly one-half of the structure of the "vuv peak" consisted of delayed gamma rays produced by beam scattering after the target, and this broader feature partially overlapped the vuv signals in time. We were able to exclude more than half of this background with our present timing resolution.

For our spectroscopy measurements, the spectrometer was positioned to view the vuv spectrum emitted from the region of the beam located immediately after the target foil. A typical set of data is shown in Fig. 4 as a two-dimensional plot of time-resolved spectra versus position on the PSD. The ridge corresponding to the vuv spectrum clearly displays the wavelength structure of highly ionized argon transitions, whereas the time-resolved ridge representing the prompt gammas has no position-dependent structure.

Argon spectra that were extracted from the data using appropriate time-window cuts are shown in Figs. 5 and 6. A total of eight such spectra were obtained, centered at three different wavelength settings for the PSD. In Fig. 5 the $1s2s\ ^3S_1-1s2p\ ^3P_0$ transition in heliumlike Ar^{16+} appears in the third order of diffraction at 1985 Å. Prom-

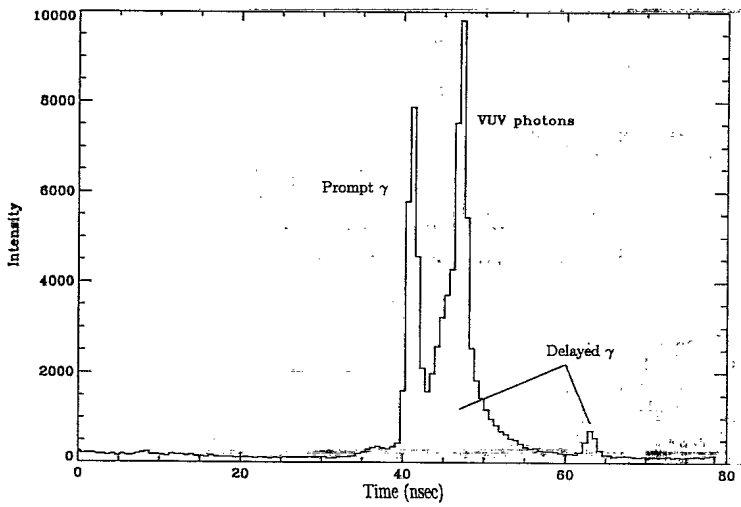

FIG. 3. Spectrum of the arrival times of detected signals. The signals are delayed in time for convenient display with respect to the 12.5-MHz reference pulse of the ion beam time structure. (Intensity is in arbitrary units.)

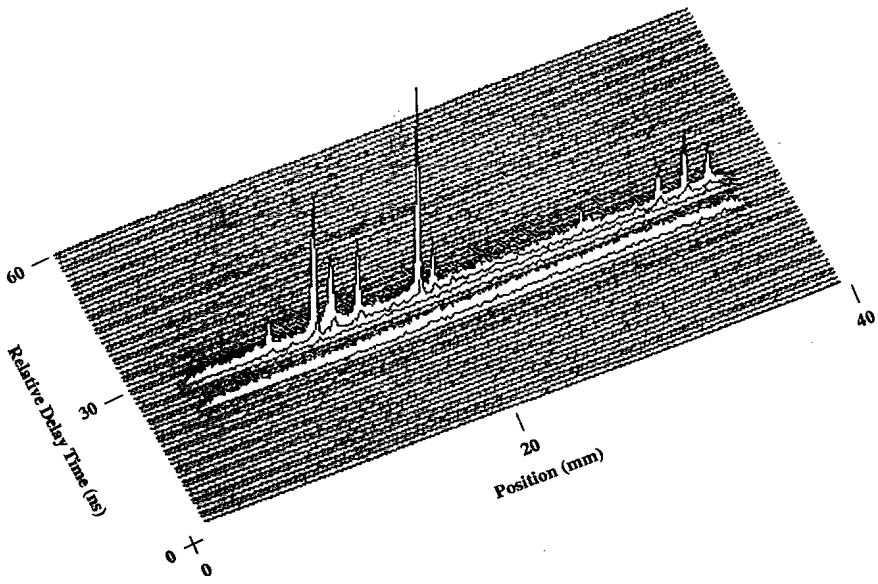

FIG. 4. Time-resolved spectra obtained using the position-sensitive detector. The spectrum of highly ionized argon is isolated in the ridge corresponding to the "vuv photon" peak in the projection displayed in Fig. 3. (Intensity is in arbitrary units.)

inent Rydberg transitions and $2s-2p$ transitions in the Ar^{14+} to Ar^{16+} ions account for all the observed lines. Several of these transitions are suitable as reference wavelengths, as discussed below. In Fig. 6, the $1s2s\ ^3S_1-1s2p\ ^3P_2$ transition appears in the fourth order of diffraction. The long lifetime of the $1s2p\ ^3P_0$ state (5.08 ns) is emphasized by the spectrum shown in Fig. 7. The target foil was displaced up-beam a distance of 2.4 cm from its position for the prompt spectra, resulting in a spectrum of the highly ionized argon emission that is delayed by 900 ps after excitation. Comparison with Fig. 5 reveals that all the shorter-lived transitions have decayed to below the $^3S_1-{}^3P_0$ intensity, which itself has decreased by only 15%.

III. WAVELENGTH DETERMINATION

The determination of an accurate wavelength scale for the heliumlike $2\ ^3S-2\ ^3P$ transitions required two procedures: the establishment of the wavelength dispersion across the PSD, and the determination of sufficiently accurate reference transition wavelengths in the beam spectra. The wavelength dispersion was established by recording a series of spectra of Ar I and Ar II transitions produced in a gas discharge lamp. The in-beam reference lines were determined primarily by accurate calculation of the structures of Rydberg transitions excited in the ion-foil interaction.

A. Wavelength dispersion

The wavelength dispersion function across the PSD was mapped in detail for each of the three wavelength regions used in the experiment. This was accomplished by tracking of relative separations of the resonance transitions of Ar I at 1048.220 and 1066.660 Å, and of Ar II at 919.781 and 932.054 Å in the second and third orders of diffraction as they were shifted stepwise across the detec-

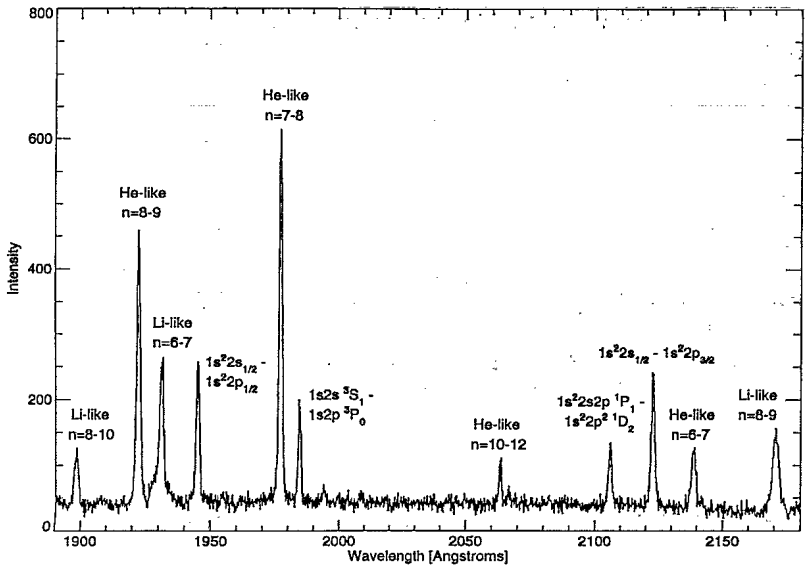

FIG. 5. Prompt spectrum of highly ionized argon showing the $1s2s\ ^3S_1-1s2p\ ^3P_0$ transition in the third order of diffraction. (Intensity is in arbitrary units.)

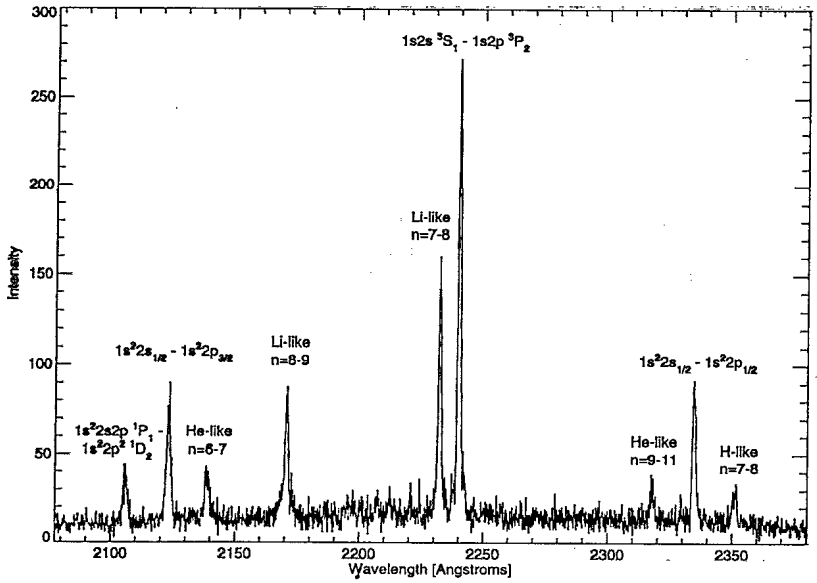

FIG. 6. Prompt spectrum of highly ionized argon showing the $1s2s\ ^3S_1-1s2p\ ^3P_2$ transition in the fourth order of diffraction. (Intensity is in arbitrary units.)

tor. About 140 separate spectra of the Ar I and II lines were recorded for each of the three wavelength regions by incrementally changing the centroid wavelength on the fixed detector for each spectrum. The localized dispersion at all positions on the PSD could then be determined by fitting the sets of slowly varying observed separations between the closely spaced pairs of resonance lines with a polynomial form. These dispersion functions for each of the three wavelength regions were corrected for time dilation effects for the fast-beam source ($\gamma=1.0043$) and then applied to the beam spectra to establish accurate separations between the reference lines and the heliumlike $^3S-^3P$ lines. For the $1s2s\ ^3S_1-1s2p\ ^3P_0$ transition at 661.5 Å, the primary reference line was the heliumlike $n=7-8$ Rydberg transition at 659.1 Å, both being observed in third order (see Fig. 5) and in fourth order (not shown). For the $1s2s\ ^3S_1-1s2p\ ^3P_2$ transition at 559.9 Å (observed in fourth order) the primary reference line was the lithiumlike $n=7-8$ Rydberg transition at 744.1 Å (observed in third order, see Fig. 6). Other Rydberg transitions in heliumlike and lithiumlike argon and the lithiumlike $2s_{1/2}-2p_{1/2,3/2}$ resonance transitions that appeared in the spectra at larger wavelength separations from the $^3S-^3P$ transitions were also included in the fits.

B. Rydberg transitions

Accurate determination of reference wavelength values in the beam spectrum requires careful analysis of Rydberg transition structures [3,10,13]. The heliumlike and lithiumlike $n=7-8$ Rydberg transitions served as our primary reference lines, since they appeared within a few Å of the respective $^3S_1-^3P_{0,2}$ transitions in the spectra. The Rydberg structure analysis involves calculation of the wavelengths and intensities of the fine-structure components that comprise the unresolved Rydberg line in the fast-beam spectrum, as described in detail below. These

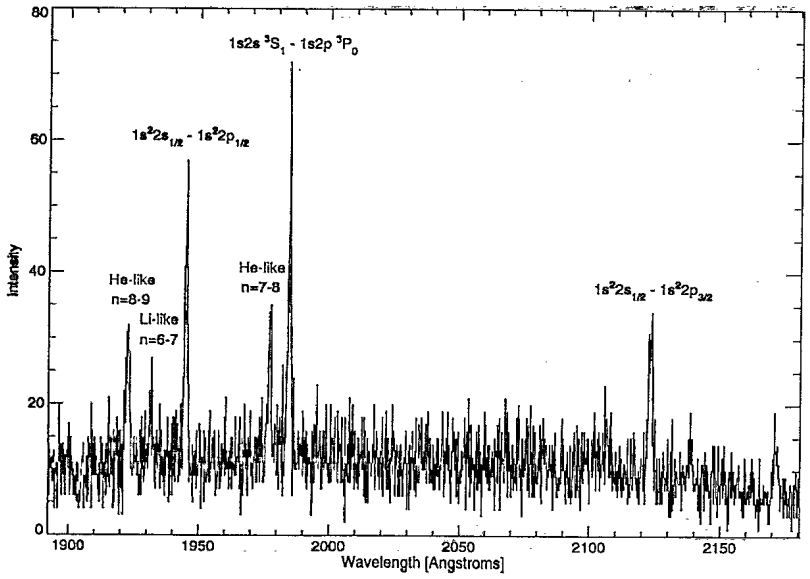

FIG. 7. Delayed spectrum of the same wavelength region as in Fig. 5, displayed 900 ps after the time of excitation. The long-lived $1s2s\ ^3S_1-1s2p\ ^3P_0$ transition is now the strongest feature in the spectrum. (Intensity is in arbitrary units.)

calculated components are modeled as Gaussian line shapes with instrumental linewidths, and then summed to provide the calculated Rydberg transition profile. The modeled profile is fit using the same function as that for the background-corrected Rydberg line in the observed spectrum, which provides an accurate calculated wavelength for that reference transition.

The wavelength structure of the Rydberg transition is accurately approximated using a core-polarization-corrected, hydrogenlike description. In the traditional approach [14], the associated Dirac fine-structure transition wavelengths are corrected by angular-momentum-dependent terms based upon an atomic core polarization model. The core polarization formulation represents a simple modeling of the long range electron-ion interaction for an unperturbed, nonpenetrating, high-angular-momentum Rydberg state [15–17]. In this model, the inner electrons in the ion core are treated as a deformable core of charge that adjusts the Rydberg state energy through parametrized core polarizability contributions. These contributions are customarily represented by a perturbative polarization correction to the hydrogenlike state term energy (magnitude of the binding energy) of the form

$$\Delta p = A\langle r^{-4}\rangle + B\langle r^{-6}\rangle ,$$

where the $\langle r^{-x}\rangle$ are radial expectation values for the corresponding hydrogenlike ion, and A and B are the atomic core parameters. Usually the associations $A=\alpha_d$ and $B=(\alpha_q-6\beta)$ are adopted, where α_d and α_q are the dipole and quadrupole polarizabilities of the core, and β is a nonadiabatic (or dynamical) correction. Thus, the polarizability contributions reflect attractive interactions, whereas the dynamical correction is repulsive. Extensions of such models to account for penetration effects, higher-order multipole polarizabilities, or higher-order relativistic corrections do not produce significant effects for the present analyses of heliumlike and lithiumlike Rydberg states. Conversely, applications of polarization model descriptions to more complicated atomic systems such as berylliumlike Rydberg state structures are known to be incomplete and less reliable [18].

An alternative description of the Rydberg transition structure [19] is provided by solving the Dirac equation using a screened central potential [20]. This nonperturbative approach directly incorporates the core-polarization contributions into the solution of the Rydberg state fine-structure energies. We have found no significant differences between the perturbative and nonperturbative methods for calculating our Rydberg transition structures. A semiempirical determination of the core-polarization parameters for heliumlike ions, described by Edlén [21], shows reasonable agreement with the above formulations based upon polarizabilities.

Relativistic calculations of dipole polarizabilities for hydrogenlike ions (the atomic cores for heliumlike Rydberg states) have been performed by Drake and Goldman [22] and quadrupole polarizabilities have been reported by Kaneko [23]. A nonrelativistic dynamical correction has been calculated by Drachman [16]. Relativistic calculations of heliumlike dipole and quadrupole polarizabilities have been performed by Johnson, Kolb, and Huang [24]. The resulting total polarization corrections to the Dirac transition wavelengths for the heliumlike and lithiumlike $n=7-8$ transitions are very small (≤ 0.01 Å) for all the more intense higher-angular-momentum components excited in the beam-foil interaction, and they are always small with respect to the Dirac structure itself. The resulting estimated polarization model contributions to the uncertainties in the Rydberg transition wavelengths are negligible for this work (see Table I).

The intensities of the polarization-corrected, Dirac fine-structure transition wavelengths used for the modeling of the Rydberg transition structures depend upon a number of experimental parameters (see Table I). The most important of these is the initial state populations resulting from the ion-foil interaction. We have considered several different population schemes, ranging from the $(2J+1)$ statistical model, which may underpopulate the high-L states, to the L^2 model, which probably overpopulates the high-L states [3]. We have used the $(2J+1)$ model in our final analysis, and have adopted the wavelength shifts of 0.0130 and 0.0104 Å between the results for the above two models as a conservative estimate of the population contributions to the two Rydberg wavelength uncertainties in Table I.

The fine-structure dependence of the Rydberg state lifetimes is reflected in the fine-structure intensities through considerations of cascade repopulation, transi-

TABLE I. Contributions to the uncertainties of the Rydberg transition reference wavelengths.

	He-like $n=7-8$ (Å)	Li-like $n=7-8$ (Å)
Beam energy	0.0002	0.0003
Cascades	0.0006	0.0013
Population	0.0130	0.0104
Polarization model	0.0004	0.0004
Transition probabilities	0.0013	0.0016
Gaussian fit	0.0011	0.0011
Linewidths	0.0013	0.0012
Beam length viewed	0.0010	0.0010
Foil position	0.0107	0.0098
Sum in quadrature	0.0170 Å	0.0145 Å

tion probabilities, beam velocity, target foil position, and observed beam length. Cascade contributions into the $n=8$ Rydberg states were modeled for all direct and indirect $E1$-allowed transitions from $n=9$ through $n=12$ states. Rapid convergence was found as higher states were included, and the size of the effect due to the $n=12$ state was adopted as the uncertainty contribution in Table I. The hydrogenic transition probabilities used in the decay scheme were varied by a conservative 10% to obtain their uncertainty contributions. The beam velocity uncertainty of $<1\%$ was not critical for these measurements and was based upon the spread of beam energy values during the experiment.

The relative intensity contributions from the shapes of the fine-structure decay profiles depend upon the integrated length of the detected beam fluorescence "window" and the position of this window with respect to the target foil. The foil position was the more important contribution, with the associated uncertainties of about 0.01 Å representing a conservative estimate of 250 μm for the foil position uncertainty. Adopting the same uncertainty for the length of beam viewed yielded a contribution of 0.001 Å.

The instrumental linewidths applied to the modeled fine-structure transition components were varied from 1.0 to 1.2 Å to produce the linewidth uncertainties in Table I. The statistical uncertainty in the fitted Gaussian centroid of the final modeled Rydberg structure was similarly about 0.001 Å.

The population and foil position contributions account for all but 2% of the sum in quadrature of the contributing uncertainties in the Rydberg transition wavelengths shown in Table I.

C. Final wavelength uncertainties

The contributions to the wavelength uncertainties for the $1s2s\ ^3S_1-1s2p\ ^3P_{0,2}$ transitions in Ar^{16+} are listed in Table II. The wavelength determinations are dominated by the uncertainties in the Rydberg transition reference wavelength values obtained from Table I. The wavelengths and fitted centroids of the Ar I and Ar II lines represent the uncertainty contributions from the wavelength dispersion determinations. Possible small doppler-shift corrections to the dispersion arise due to uncertainty in the detection angle of $90.0\pm0.3°$ between the optic axis of the spectrometer and the beam axis. The fit reproducibility in Table II is the standard deviation of the mean of the six measurements of the $^3S_1-^3P_0$ transition and the four measurements of the $^3S_1-^3P_2$ transition. The sums in quadrature yield final uncertainties of 0.0182 and 0.0157 Å for the $^3S_1-^3P_0$ and $^3S_1-^3P_2$ transition wavelengths, respectively.

IV. RESULTS

The final results for our measured transition wavelengths in heliumlike Ar^{16+} are 559.944(16) Å for $1s2s\ ^3S_1-1s2p\ ^3P_2$ and 661.533(18) Å for $1s2s\ ^3S_1-1s2p\ ^3P_0$. These represent measurements at the 27 and 29 ppm levels, respectively. We compare our results with calculations and with previous measurements for Ar^{16+} in Table III and in Figs. 8 and 9. Our result for the $^3S_1-^3P_0$ transition disagrees substantially with that for the recoil-ion measurement [11]. Our result for the $^3S_1-^3P_2$ transition improves upon the previous precision [11] by a factor of 6. The measured values are sensitive to the relativistic contributions to 140 and 450 ppm for the $^3P_2$ and $^3P_0$ transitions, respectively, and they test the total QED corrections to 0.45 and 0.35%, using the designations of Drake [2]. The $^3P_2-^3P_0$ fine structure interval is determined to 230 ppm.

Our experimental results show best agreement with the new many-body and CI calculations [7–9] for both of the fine-structure transitions in Ar^{16+}. Note that all three recent calculations include corrections for QED and mass-polarization effects taken from Drake [2]. For the $^3P_2$ transition, the variational-perturbation calculations [2,3] agree with these newer theoretical results to within a few cm^{-1}, whereas the two MCDF values [4,5] disagree by 20–30 cm^{-1}. For the $^3P_0$ transition, all the earlier calculations disagree with the newer theoretical results by more than 20 cm^{-1}. In particular, our measured discrepancy of -22 ± 4 cm^{-1} from the unified value of Drake [2] represents a measurement of the relativistic and QED terms of order $(Z\alpha)^4$ a.u. and higher that were not included in that calculation.

V. DISCUSSION

The new generation of relativistic calculations of $n=2$ state energies in heliumlike ions that has appeared over the past two years [7–9] has established significantly improved benchmarks of theoretical accuracy in our understanding of the two-electron atomic system. The most dramatic aspect of these calculations is the removal of

TABLE II. Contributions to the uncertainties of the $1s2s\ ^3S_1-1s2p\ ^3P_{0,2}$ transitions wavelengths.

	$^3S_1-^3P_0$ (Å)	$^3S_1-^3P_2$ (Å)
Centroid of Ar I and Ar II lines	0.0037	0.0037
Wavelengths of Ar I and Ar II lines	0.0003	0.0003
Wavelength of Rydberg transition	0.0170	0.0145
Beam energy	0.0005	0.0005
Detection angle	0.0020	0.0020
Fit reproducibility	0.0051	0.0044
Sum in quadrature	0.0182 Å	0.0157 Å

TABLE III. Calculated and measured energies (cm^{-1}) for the $1s2s\ ^3S_1-1s2p\ ^3P_{0,2}$ transitions and the $2p\ ^3P_{2-0}$ fine structure interval in heliumlike argon.

	Ref.	$^3S_1-^3P_0$	$^3S_1-^3P_2$	$^3P_2-^3P_0$
		Theory		
DeSerio *et al.*	[3]	151 189	178 574	27 385
Hata and Grant	[4]	151 179	178 558	27 379
Indelicato	[5]	151 130	178 546	27 416
Drake	[2]	151 186	178 577	27 391
Johnson and Sapirstein	[7]	151 155	178 576	27 421
Chen, Cheng, and Johnson	[8]	151 156	178 578	27 422
Plante, Johnson, and Sapirstein	[9]	151 155	178 576	27 421
		Experiment		
Davis and Marrus	[10]	151 350(250)	178 510(290)	27 160
Beyer, Folkmann, and Schartner	[11]	151 203.6(9.1)	178 591(32)	27 387
This work		151 164.0(4.1)	178 589.3(5.1)	27 425.3(6.5)

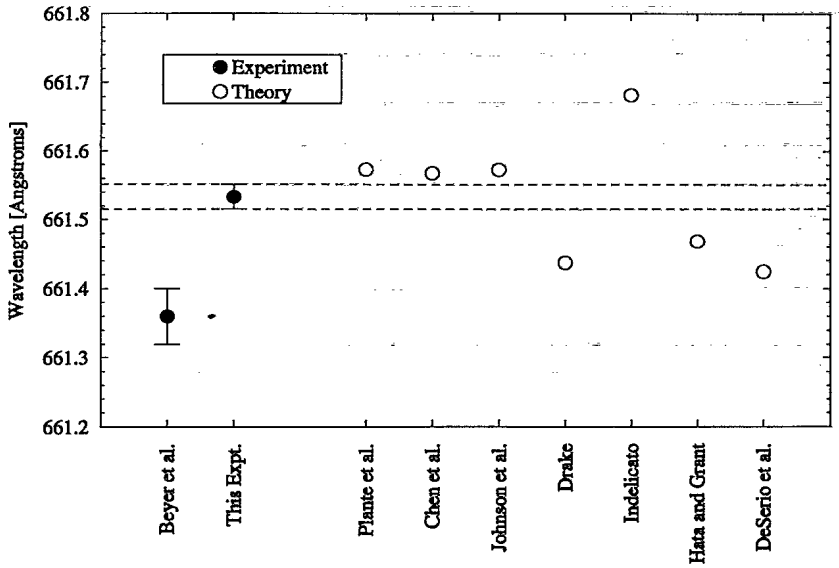

FIG. 8. Comparison of our wavelength result for the $1s2s\ ^3S_1-1s2p\ ^3P_0$ transition in Ar^{16+} with the previous measurement and with calculations.

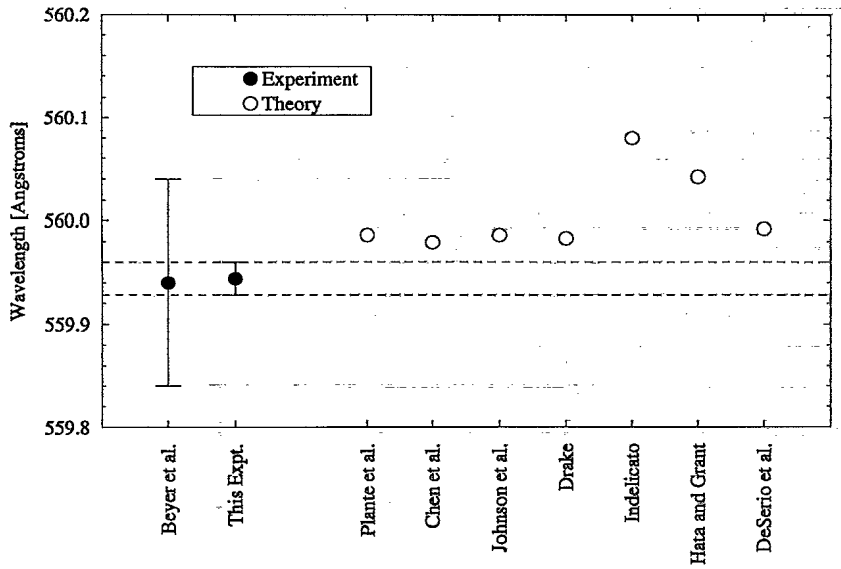

FIG. 9. Comparison of our wavelength result for the $1s2s\ ^3S_1-1s2p\ ^3P_2$ transition in Ar^{16+} with the previous measurement and with calculations.

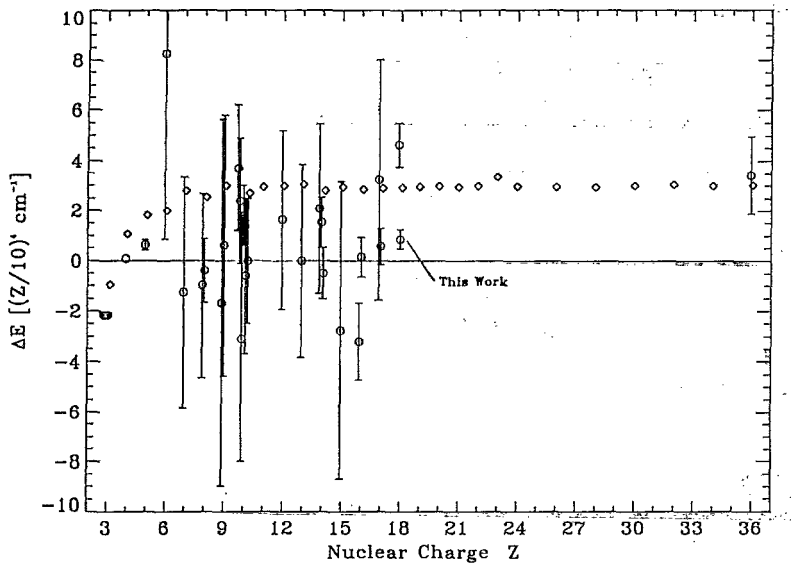

FIG. 10. Comparison of experiment and theory with respect to the MBAO calculations of Plante, Johnson, and Sapirstein [9] for the scaled $1s2s\ ^3S_1-1s2p\ ^3P_0$ transition energy in heliumlike ions. The unified calculations of Drake [2] are shown as diamonds.

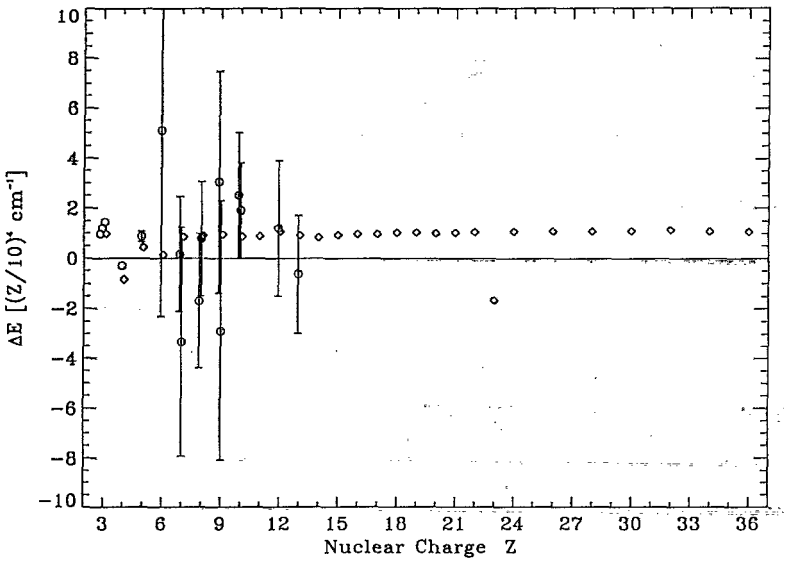

FIG. 11. Comparison of experiment and theory with respect to the MBAO calculations of Plante, Johnson, and Sapirstein [9] for the scaled $1s2s\ ^3S_1-1s2p\ ^3P_1$ transition energy in heliumlike ions. The unified calculations of Drake [2] are shown as diamonds.

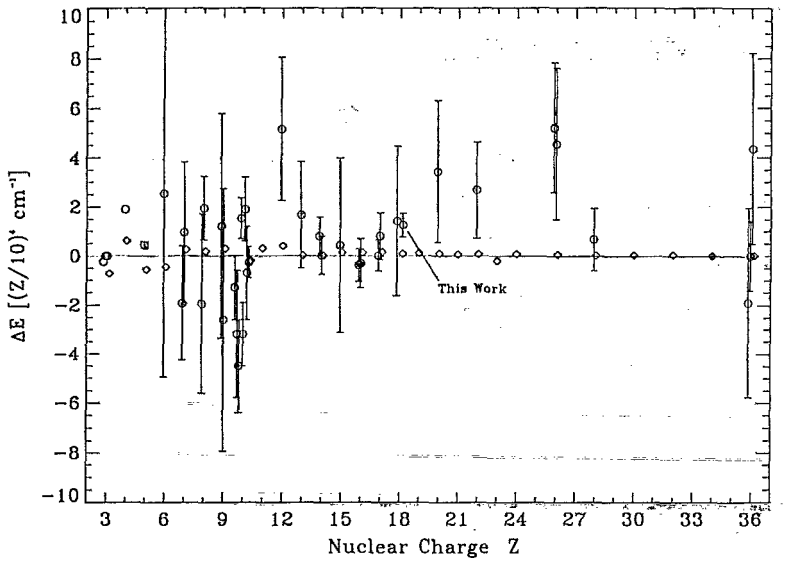

FIG. 12. Comparison of experiment and theory with respect to the MBAO calculations of Plante, Johnson, and Sapirstein [9] for the scaled $1s2s\ ^3S_1-1s2p\ ^3P_2$ transition energy in heliumlike ions. The unified calculations of Drake [2] are shown as diamonds.

TABLE IV. Experimental transition energies (in cm^{-1}) for the $1s2s\ ^3S_1-1s2p\ ^3P_{0,1,2}$ transitions in heliumlike ions. New measurements by Riis *et al.* [Phys. Rev. A **49**, 207 (1994)] have recently been reported for $Z=3$: 18 231.301 97(2), 18 226.108 24(2), and 18 228.198 96(2) cm^{-1} for the $J=0$, 1, and 2 transitions, respectively.

Z	$1s2s\ ^3S_1-1s2p\ ^3P_0$	$1s2s\ ^3S_1-1s2p\ ^3P_1$	$1s2s\ ^3S_1-1s2p\ ^3P_2$	Ref.
3	18 231.302 8(8)	18 226.109 3(7)	18 228.199 9(3)	[25]
	18 231.303 0(12)	18 226.108 2(12)	18 228.197 9(12)	[26]
	18 231.301 88(19)	18 226.112 06(21)	18 228.199 35(25)	[27]
4	26 867.29(72)	26 856.03(72)	26 871.26(72)	[28]
	26 864.40(22)	26 852.85(22)	26 867.72(22)	[29]
		2 6852.35	2 6867.21	[30]
	26 864.612 0(4)	26 853.0534(3)	26 867.9484(3)	[31]
5	35 393.26			[32]
	35 393.39(38)	35 376.98(38)	35 429.76(38)	[33]
		35 377.23	35 429.51	[30]
	35 393.627(13)	35 377.424(13)	35 430.084(9)	[34]
6	43 899.77(96)	43 886.86(96)	44 022.33(97)	[32]
			44 022.52	[35]
7	52 414.47	52 429.04	52 719.82	[36]
	52 413.9(1.4)	52 429.04(55)	52 719.54(56)	[37]
	52 420.0(1.1)	52 428.2(1.1)	52 720.23(69)	[38]
8	60 991.2(3.0)	61 051.6(3.0)	61 603.3(3.0)	[39]
	60 980.4(3.0)	61 038.9(3.0)	61 590.4(3.0)	[40]
	60 979.3(3.0)	61 040.74(75)	61 595.32(76)	[37]
	60 983.8(1.1)		61 593.8(1.5)	[35]
	60 978.2(1.5)	61 036.6(1.1)	61 588.1(1.5)	[41]
	60 978.44(52)	61 037.62(93)	61 589.70(53)	[38]
9	69 586.0(2.9)	69 743.8(2.9)	70 700.4(3.0)	[40]
	69 589.4(4.8)		70 705.9(3.0)	[41]
	69 590.9(3.4)	69 739.9(3.4)	70 697.9(3.5)	[42]
10	78 266.9(2.5)	78 566.3(2.5)	80 120.5(1.3)	[40]
	78 265.6(2.5)		80 118.6(2.6)	[43]
	78 260.1(4.9)		80 117.3(1.9)	[44]
			80 126.3(5.8)	[44]
	78 265.0(1.2)	78 565.7(1.9)	80 123.33(83)	[38]
			80 118.6(1.3)	[45]
			80 123.7(1.3)	[11]
	78 262.6(3.1)		80 121.1(1.9)	[46]
	78 263.2(2.5)		80 121.53(64)	[47]
12	95 850.6(7.4)	96 682.8(5.6)	100 262.7(6.0)	[42]
13	104 930(110)		111 110(120)	[48]
	104 778(11)	106 023.2(6.7)	111 156.8(6.2)	[42]
14	113 856(78)		122 775(60)	[49]
	113 817(13)		122 730(15)	[50]
	113 790(25)		122 745(15)	[51]
	113 814.9(3.9)		122 746.1(3.0)	[3]
	113 807.1(3.9)		122 743.1(3.0)	[52]
15	122 941(30)		135 153(18)	[53]
16	132 200(40)		148 480(20)	[51]
	132 198(10)		148 493.5(4.4)	[3]
	132 222(5)		148 496(5)	[54]

TABLE IV. (*Continued*).

Z	$1s2s\ ^3S_1-1s2p\ ^3P_0$	$1s2s\ ^3S_1-1s2p\ ^3P_1$	$1s2s\ ^3S_1-1s2p\ ^3P_2$	Ref.
17	141 672(15)		162 912.9(3.5)	[13]
	141 707(30)		162 912.9(5.8)	[55]
			162 920(25)	[51]
	141 643(40)		162 922.2(5.3)	[3]
	141 621(5)		162 929(5)	[54]
18	151 350(250)		178 510(290)	[10]
	151 203.6(9.1)		178 591(32)	[11]
	151 164.0(4.1)		178 589.3(5.1)	This work
20			214 225(46)	[56]
22			256 746(46)	[57]
24			307 350(470)	[58]
26			368 730(820)	[59]
			368 980(120)	[60]
			368 950(140)	[61]
28			441 950(78)	[62]
29	267 950(360)		483 910(190)	[63]
36			899 690(650)	[64]
	357 400(260)		900 010(240)	[65]
			900 740(650)	[66]
54			3 751 000(14000)	[67]

the previously dominant energy uncertainty [2] that was due to uncalculated relativistic corrections of order $(Z\alpha)^4$ a.u., and the identification of the strong fine-structure dependence of these corrections. These nonradiative contributions to the $n=2$ triplet state energies are now calculated for low Z and intermediate Z ions to an accuracy of 10^{-7} to 10^{-5} a.u., or ≤ 1 cm^{-1}, and for high Z ions to 10^{-5} to 10^{-4} a.u. [9]. Our experimental results for the $1s2s\ ^3S_1-1s2p\ ^3P_0$ transition energy in Ar^{16+} reveals a discrepancy of $(-1.0\pm0.2)\times10^{-4}$ a.u. from the earlier unified calculations [2] that accounts for about 70% of the new order-$(Z\alpha)^4$ relativistic corrections for $Z=18$ in the recent calculations [7–9]. The remaining differences in transition energies between our measurements and the three new calculations are 9 ± 4 cm^{-1} for $^3S_1-{}^3P_0$ and 12 ± 5 cm^{-1} for $^3S_1-{}^3P_2$. These differences are significant at the level of a little better than 2σ, and they are of equal magnitude and sign. Thus, our measurements suggest the existence of uncalculated QED contributions for $Z=18$ of magnitude about 10 cm^{-1} (or 4.5×10^{-5} a.u.) in the $1s2s\ ^3S_1$ energy, which is the common lower state in the transitions. Such determinations of uncalculated QED terms of order $(Z\alpha)^4$ a.u. represent the most interesting theoretical problem remaining for the helium isoelectronic sequence [9].

We compare our results for the $1s2s\ ^3S_1-1s2p\ ^3P_{0,2}$ fine-structure transition energies in Ar^{16+} with previous measurements and with calculations for the isoelectronic sequence of heliumlike ions in Figs. 10–12. The $1s2s\ ^3S_1-1s2p\ ^3P_1$ transition is included for completeness. The data are plotted with respect to the most recent of the accurate calculations, the MBAO results of Plante, Johnson, and Sapirstein [9]. These calculations show excellent agreement with the recent MBPT [7] ($Z\geq10$) and CI [8] ($Z\geq5$) calculations. The earlier unified results of Drake [2] are included in Figs. 10–12 to emphasize the strong fine-structure dependence of the newly calculated relativistic contributions in Refs. [7–9]. The Z^4 scaling of the plots is chosen to reveal the nearly constant Z^4-dependent magnitudes of these new relativistic corrections in each transition energy for $Z=10$–36. The largest such contribution appears in the $^3S_1-{}^3P_0$ transition as a decrease in the energy of the $^3P_0$ state by about $3(Z/10)^4$ cm^{-1}. A similar contribution of about one-third this magnitude appears for the $^3P_1$ state, and there is an order of magnitude smaller correction for the $^3P_2$ state. The relativistic contributions grow somewhat more strongly for $Z>36$, as discussed in Ref. [8]. For $Z\leq6$, the Z-dependent scatter that appears in the high-precision laser fluorescence data points in Figs. 10–12 probably reflects numerical inaccuracy in the low-Z MBAO results [9], chosen as our reference calculation for the plots. The estimated theoretical uncertainties for $Z=3$–5 for all the accurate low-Z calculations (taken from Ref. [9], including updated values from Drake) range from about $\pm(1-4)\times(Z/10)^4$ cm^{-1}, and they overlap all the precision laser fluorescence measurements for these low-Z ions.

We list in Table IV all direct experimental measurements of the $1s2s\ ^3S-1s2p\ ^3P$ transition energies for $Z=4$–54, as well as laser-based measurements for $Z=3$. Recent high-precision theoretical and experimental studies of these transitions in the neutral helium atom have been discussed in Refs. [68] and [69], and are omitted here. For clarity we have excluded from Figs. 10–12 those experimental results for which the magnitude of ei-

ther the plotted value or the uncertainty would exceed $10(Z/10)^4$ cm^{-1}, as well as early less precise values for $Z<6$. We have also excluded several indirect measurements of $2s-2p$ energy structures at higher Z that have been obtained from $2p\ ^3P$ state lifetime measurements, which were discussed in Ref. [6]. We note that all published measurements of heliumlike atomic structure for $Z>10$, with the exception of the recoil-ion study [11] discussed above, are beam-foil spectroscopy measurements.

Most of the recent precise measurements for the $^3S_1-^3P_{0,2}$ transition energies for $Z>5$ show reasonable agreement with the new many-body and CI calculations. However, the measurements do not exclude the existence of uncalculated energy contributions of order $0.1(Z\alpha)^4$ a.u. in magnitude. Since the new calculations are expected to account for nonradiative contributions to an accuracy of $\leq 0.01(Z\alpha)^4$ a.u. for $Z>10$, the remaining uncalculated corrections must reside in the higher-order QED terms. Our measurements for $Z=18$ display a small systematic discrepancy from the new calculations that is consistent with a reduction in the QED contribution to the $1s2s\ ^3S_1$ state energy by about $0.15(Z\alpha)^4$ a.u., a 1% correction to the QED effects.

VI. CONCLUSION

We have measured the wavelengths of the $1s2s\ ^3S_1-1s2p\ ^3P_{0,2}$ fine-structure transitions in the heliumlike Ar^{16+} ion with a precision of <30 ppm. The experimental results are sensitive to recently calculated $(Z\alpha)^4$-dependent relativistic corrections to the $n=2$ state energies that represent a new benchmark in our knowledge of the atomic structure of heliumlike ions. Our measurements of the fine-structure transition energies, coupled with the accurate new calculations of nonradiative contributions and the existing lower-order QED calculations, establish an upper limit to the magnitude of uncalculated higher-order QED corrections for $Z=18$. Our results suggest that the inclusion of such higher-order terms will reduce the calculated QED contributions to the $1s2s\ ^3S_1$ energy for Ar^{16+} by about 4.5×10^{-5} a.u., or $0.15(Z\alpha)^4$ a.u. This modification of the QED correction for the $1s2s\ ^3S_1$ state is consistent with the results of new QED calculations [70] for the $n=1$ and $n=2$ singlet states in heliumlike ions.

Our spectroscopic measurements establish the need for explicit calculations of higher-order QED terms for the $n=2$ triplet states of heliumlike ions as the next refinement in the new generation of accurate understanding of two-electron atomic systems. Further experimental confirmation of the size of the uncalculated QED contributions suggested by our measurements will require additional measurements of $2\ ^3S-2\ ^3P$ transition energies with precisions of $<0.1(Z\alpha)^4$ a.u.

Note added. Following submission of this paper, a study of recoil-ion spectra of argon was published [Hallett, Howie, Silver, and Dietrich, Phys. Lett. A **192**, 43 (1994)] in which wavelength values of 559.95(2) Å and 661.58(2) Å have been suggested for the $1s2s\ ^3S_1-1s2p\ ^3P_{2,0}$ transition energies, respectively, in Ar^{16+}. The identifications of the weak Ar^{16+} lines amid many unidentified lines in the recoil-ion spectra were based upon approximate agreements with theoretical wavelengths. The $^3P_2-^3P_0$ fine structure interval of 27 434(7) cm^{-1} determined by the new studies disagrees by 2σ with the accurately established theoretical interval of 27 421 cm^{-1} [Refs. 7–9] (see Table III), which is expected to be only weakly sensitive to uncalculated QED contributions for $n=2$ triplet states.

ACKNOWLEDGMENTS

We are grateful to the ATLAS staff and to C. Kurtz and B. J. Zabransky for excellent technical assistance during this experiment. We thank W. R. Johnson and J. Sapirstein for helpful discussions on the heliumlike calculations. This work was supported by the U.S. Department of Energy, Office of Basic Energy Sciences, Division of Chemical Sciences, under Grant No. DE-FG02-92ER14283 (University of Notre Dame), Grant No. DE-FG05-88ER13958 (University of Toledo), and Contract No. W-31-109-ENG-38 (Argonne National Laboratory).

[1] Y. Accad, C. L. Pekeris, and B. Schiff, Phys. Rev. A **4**, 516 (1971).
[2] G. W. F. Drake, Can. J. Phys. **66**, 586 (1988).
[3] R. DeSerio, H. G. Berry, R. L. Brooks, J. Hardis, A. E. Livingston, and S. J. Hinterlong, Phys. Rev. A **24**, 1872 (1981).
[4] J. Hata and I. P. Grant, J. Phys. B **16**, 523 (1983); **17**, 931 (1984).
[5] P. Indelicato, Nucl. Instrum. Methods Phys. Res. Sect. B **31**, 14 (1988); P. Indelicato, O. Gorceix, and J. P. Desclaux, J. Phys. B **20**, 651 (1987); P. Indelicato, F. Parente, and R. Marrus, Phys. Rev. A **40**, 3505 (1989).
[6] H. G. Berry, R. W. Dunford, and A. E. Livingston, Phys. Rev. A **47**, 698 (1993).
[7] W. R. Johnson and J. Sapirstein, Phys. Rev. A **46**, R2197 (1992).
[8] M. H. Chen, K. T. Cheng, and W. R. Johnson, Phys. Rev. A **47**, 3692 (1993).
[9] D. R. Plante, W. R. Johnson, and J. Sapirstein, Phys. Rev. A **49**, 3519 (1994).
[10] W. A. Davis and R. Marrus, Phys. Rev. A **15**, 1963 (1977).
[11] H. F. Beyer, F. Folkmann, and K.-H. Schartner, Z. Phys. D **1**, 65 (1986).
[12] J. O. Stoner and J. A. Leavitt, Appl. Phys. Lett. **18**, 477 (1971); J. A. Leavitt, J. W. Robson, and J. O. Stoner, Nucl. Instrum. Methods **110**, 423 (1973).
[13] H. G. Berry, R. DeSerio, and A. E. Livingston, Phys. Rev. Lett. **41**, 1652 (1978).
[14] B. Edlén, in *Handbuch der Physik*, edited by S. Flügge (Springer, Berlin, 1964), Vol. XXVII, pp. 80–220; see, also, K. Bockasten, Ark. Fys. **10**, 567 (1956), where historical references to applications of the polarization concept to atomic structure may be found.
[15] L. J. Curtis, Phys. Scr. **35**, 805 (1987).
[16] R. J. Drachman, Phys. Rev. A **26**, 1228 (1982).
[17] R. R. Freeman and D. Kleppner, Phys. Rev. A **14**, 1614

(1976).
[18] F. G. Serpa and A. E. Livingston, Phys. Rev. A **43**, 6447 (1991).
[19] E. J. Galvez, A. E. Livingston, A. J. Mazure, H. G. Berry, L. Engström, J. E. Hardis, L. P. Somerville, and D. Zei, Phys. Rev. A **33**, 3667 (1986).
[20] W. R. Johnson (private communication).
[21] B. Edlén, Phys. Scr. **19**, 225 (1979).
[22] G. W. F. Drake and S. P. Goldman, Phys. Rev. A **23**, 2093 (1981).
[23] S. Kaneko, J. Phys. B **10**, 3347 (1977).
[24] W. R. Johnson, D. Kolb, and K.-N. Huang, At. Data Nucl. Data Tables **28**, 333 (1983).
[25] R. Bayer, J. Kowalski, R. Neumann, S. Noehte, H. Suhr, K. Winkler, and G. zu Putlitz, Z. Phys. A **292**, 329 (1979); M. Englert, J. Kowalski, F. Mayer, R. Neumann, S. Noethe, R. Schwarzwald, H. Suhr, K. Winkler, and G. zu Putlitz, Appl. Phys. B **28**, 81 (1982).
[26] R. A. Holt, S. D. Rosner, T. D. Gaily, and A. G. Adam, Phys. Rev. A **22**, 1563 (1980); **29**, 1544 (1984).
[27] E. Riis, H. G. Berry, O. Poulsen, S. A. Lee, and S. Y. Tang, Phys. Rev. A **33**, 3023 (1986).
[28] M. Eidelsberg, J. Phys. B **5**, 1031 (1972).
[29] B. Löfstrand, Phys. Scr. **8**, 57 (1973).
[30] B. Edlén, Nova Acta Regiae Soc. Sci. Ups. IV **9**, (6), 30 (1934).
[31] T. J. Scholl, R. Cameron, S. D. Rosner, L. Zhang, R. A. Holt, C. J. Sansonetti, and J. D. Gillapsy, Phys. Rev. Lett. **71**, 2188 (1993).
[32] B. Edlén, Ark. Fys. **4**, 441 (1952); B. Edlén and B. Löfstrand, J. Phys. B **3**, 1380 (1970).
[33] M. Eidelsberg, J. Phys. B **7**, 1476 (1974).
[34] T. P. Dinneen, N. Berrah-Mansour, H. G. Berry, L. Young, and R. C. Pardo, Phys. Rev. Lett. **66**, 2859 (1991).
[35] G. D. Sandlin, G. F. Brueckner, and R. Tousey, Astrophys. J. **214**, 898 (1977).
[36] K. Bockasten, R. Hallin, K. B. Johansson, and P. Tsui, Phys. Lett. **8**, 181 (1964).
[37] S. C. Baker, J. Phys. B **6**, 709 (1973).
[38] N. J. Peacock, M. F. Stamp, and J. D. Silver, Phys. Scr. **T8**, 10 (1984).
[39] R. C. Elton, Astrophys. J. **148**, 573 (1967).
[40] W. Engelhardt and J. Sommer, Astrophys. J. **167**, 201 (1971).
[41] M. F. Stamp, I. A. Armour, N. J. Peacock, and J. D. Silver, J. Phys. B **14**, 3551 (1981).
[42] H. A. Klein, F. Moscatelli, E. G. Myers, E. H. Pinnington, J. D. Silver, and E. Träbert, J. Phys. B **18**, 1483 (1985).
[43] G. D. Sandlin and R. Tousey, Astrophys. J **227**, L107 (1979).
[44] H. A. Klein, S. Bashkin, B. P. Duval, F. Moscatelli, J. D. Silver, H. F. Beyer, and F. Folkmann, J. Phys. B **15**, 4507 (1982).
[45] J. S. Brown, C. W. Band, E. C. Finch, R. A. Holt, H. A. Klein, J. Laursen, A. F. McClelland, N. J. Peacock, J. D. Silver, M. F. Stamp, and J. Takacs, Nucl. Instrum. Methods Phys. Res. Sect. B **9**, 682 (1985).
[46] H. G. Berry and J. E. Hardis, Phys. Rev. A **33**, 2778 (1986).
[47] W. A. Hallett, D. D. Dietrich, and J. D. Silver, Phys. Rev. A **47**, 1130 (1993).
[48] B. Denne, S. Huldt, J. Pihl, and R. Hallin, Phys. Scr. **22**, 45 (1980).
[49] R. O'Brien, J. D. Silver, N. A. Jelley, S. Bashkin, E. Träbert, and P. H. Heckmann, J. Phys. B **12**, L41 (1979).
[50] I. A. Armour, E. G. Myers, J. D. Silver, and E. Träbert, Phys. Lett. **75A**, 45 (1979).
[51] A. E. Livingston, S. J. Hinterlong, J. A. Poirier, R. DeSerio, and H. G. Berry, J. Phys. B **13**, L139 (1980).
[52] D. J. H. Howie, W. A. Hallett, E. G. Myers, D. D. Dietrich, and J. D. Silver, Phys. Rev. A **49**, 4390 (1994).
[53] A. E. Livingston and S. J. Hinterlong, Nucl. Instrum. Methods **202**, 103 (1982).
[54] A. E. Livington, E. J. Galvez, and A. S. Zacarias (unpublished).
[55] H. G. Berry, R. DeSerio, and A. E. Livingston, Phys. Rev. A **22**, 998 (1980).
[56] S. J. Hinterlong and A. E. Livingston, Phys. Rev. A **33**, 4378 (1986).
[57] E. J. Galvez, A. E. Livingston, A. J. Mazure, H. G. Berry, L. Engström, J. E. Hardis, L. P. Somerville, and D. Zei, Phys. Rev. A **33**, 3667 (1986).
[58] J. P. Grandin, M. Huet, X. Husson, D. Lecler, D. Touvet, J. P. Buchet, M. C. Buchet-Poulizac, A. Denis, J. Desesquelles, and M. Druetta, J. Phys. (Paris) **45**, 1423 (1984).
[59] D. D. Dietrich, J. A. Leavitt, S. Bashkin, J. G. Conway, H. Gould, D. MacDonald, R. Marrus, B. M. Johnson, and D. J. Pegg, Phys. Rev. A **18**, 208 (1978).
[60] J. P. Buchet, M. C. Buchet-Poulizac, A. Denis, J. Désesquelles, M. Druetta, J. P. Grandin, and X. Husson, Phys. Rev. A **23**, 3354 (1981).
[61] J. P. Buchet, M. C. Buchet-Poulizac, A. Denis, J. Désesquelles, M. Druetta, E. J. Knystautas, and D. Lecler, Nucl. Instrum. Methods **202**, 79 (1982).
[62] A. S. Zacarias, A. E. Livingston, Y. N. Lu, R. F. Ward, H. G. Berry, and R. W. Dunford, Nucl. Instrum. Methods Phys. Res. Sect. B **31**, 41 (1988); A. E. Livingston, J. Phys. (Paris) Colloq. **50**, C1-255 (1989).
[63] J. P. Buchet, M. C. Buchet-Poulizac, A. Denis, J. Desesquelles, M. Druetta, J. P. Grandin, X. Husson, D. Lecler, and H. F. Beyer, Nucl. Instrum. Methods Phys. Res. Sect. B **9**, 645 (1985).
[64] S. Martin, J. P. Buchet, M. C. Buchet-Poulizac, A. Denis, M. Druetta, J. Désesquelles, J. P. Grandin, D. Hennecart, X. Husson, D. Lecler, and I. Lesteven, Phys. Rev. A **35**, 2327 (1987).
[65] S. Martin, A. Denis, M. C. Buchet-Poulizac, J. P. Buchet, and J. Désesquelles, Phys. Rev. A **42**, 6570 (1990).
[66] R. Büttner, B. Kraus, M. Nicolai, K. H. Schartner, F. Folkmann, P. H. Mokler, and G. Möller, in *The Physics of Highly Charged Ions,* edited by P. Richard, M. Stockli, C. L. Cocke, and C. D. Lin, AIP Conf. Proc. No. 274 (AIP, New York, 1993), p. 423.
[67] S. Martin, J. P. Buchet, M. C. Buchet-Poulizac, A. Denis, J. Desesquelles, M. Druetta, J. P. Grandin, D. Hennecart, X. Husson, and D. Lecler, Europhys. Lett. **10**, 645 (1989).
[68] T. Zhang and G. W. F. Drake, Phys. Rev. Lett. **72**, 4078 (1994).
[69] D. Shiner, P. Dixson, and P. Zhao, Phys. Rev. Lett. **72**, 1802 (1994).
[70] K. T. Cheng, M. H. Chen, W. R. Johnson, and J. Sapirstein, Phys. Rev. A **50**, 247 (1994).